

Liquid-Phase Mass Transfer in Fixed and Fluidized Beds of Large Particles

Siddh N. Upadhyay¹ and Gopal Tripathi

Department of Chemical Engineering, Institute of Technology, Banaras Hindu University, Varanasi 221005, India

Liquid-phase mass-transfer coefficients from fixed and fluidized beds of cylindrical and modified cylindrical pellets of benzoic acid are measured in the N_{Re}'' range of 0.405–11,610. Correlations are proposed for the entire liquid-solid range.

Mass transfer in fixed and fluidized beds of particles is encountered in many chemical engineering processes. Considerable experimental information on this subject has been reported in the literature over the past 30 years. The volume of this information is very large, and a complete summary has been given elsewhere (21).

For the most part, the measurements in this field are concerned with the estimation of mass-transfer rates in systems involving gases. The measurements with liquids are mainly concerned with fixed beds, and relatively few data are available for liquid fluidized beds, particularly of large particles. The results are normally correlated in terms of the Chilton-Colburn (2) J_d factor and a particle Reynolds number. In some cases, the Sherwood number has also been used. The exponent on the Schmidt group in the J_d factor is usually $2/3$; however, in certain cases 0.58 has also been used (3, 8, 23). The particle Reynolds numbers used are:

$$N_{Re} = D_p G / \mu \quad (1)$$

$$N_{Re}' = D_p G / \mu \epsilon \quad (2)$$

$$N_{Re}'' = D_p G / \mu (1 - \epsilon) \quad (3)$$

Many workers have pointed out the merits and demerits of the above three Reynolds numbers and their suitability for various cases.

The present work extends the liquid-phase mass-transfer data for fixed and fluidized beds of large particles. It covers a particle Reynolds number, N_{Re}'' range of 0.405–11,610. The experimental program is concerned with obtaining mass-transfer data for the dissolution of the compressed pellets of benzoic acid in water. On the basis of the present as well as available published data on identical systems, an attempt has also been made to verify the exponent on the Schmidt group and to judge the suitability of the three particle Reynolds numbers in correlating the mass-transfer data for random packed and fluidized beds.

Experimental

The pellets were made by compressing 35–65 mesh size grains of BDH chemically pure benzoic acid in a "Manesty" single-punch pelleting machine using eight different sets of dies and punches. The pellets were quite strong, smooth, and sharp-edged. These were freed from the surface dust by washing with water and were dried in a desiccator to constant weight before being used for the actual run. The properties of the pellets are listed in Table I.

A schematic diagram of the experimental setup used is shown in Figure 1. Water from a constant head stainless-

steel tank was pumped by means of a centrifugal pump and metered through the rotameters to the test column. A bypass at the discharge side of the pump was provided for better flow control. Metered water from the rotameters flowed past a thermometer, capable of reading up to $1/10$ of a degree centigrade, before entering the main column. After passing through the bed in the column, water was discharged through a combination of ditching and sampling line.

Another thermometer, capable of reading up to $1/10$ of a degree centigrade, was installed near the exit end of the test column, for indicating the temperature of the outgoing stream. Four different test columns of i.d. 3.901, 4.558, 6.95, and 7.220 cm were used. Each column was made of a Pyrex glass tube about 100 cm in length. Details of a test column and bed arrangement are shown in Figure 2. In the case of 6.95 and 7.22-cm i.d. columns, the two end joints were flanged in place of cone-socket joints.

In the first, third, and fourth set of measurements, the pellets weighed to the nearest 0.05 mg were placed in

Table I. Characteristics of Particles

S no.	Shape, cm	Geo-metric surface area, A_p , cm ²	Volume, V_p , cm ³	Equip diam, D_p , cm	Density, g/cm ³
1	Flat-end ^a	4.5075	0.6240	1.1968	1.2849
2	Flat-end	3.9410	0.4296	1.1210	1.2860
3	Flat-end	2.5290	0.2604	0.8973	1.3110
4	Flat-end	2.3780	0.2728	0.8701	1.2650
5	Flat-end	2.2730	0.1990	0.8505	1.2901
6	Flat-end	2.2780	0.2002	0.8517	1.3110
7	Flat-end	2.0380	0.2007	0.8061	1.2420
8	Flat-end	1.8820	0.1595	0.7743	1.3010
9	Dished-end ^b	2.3060	0.2412	0.8569	1.3010
10	Dished-end	1.1150	0.0900	0.5967	1.2250

^a □, ^b ○.

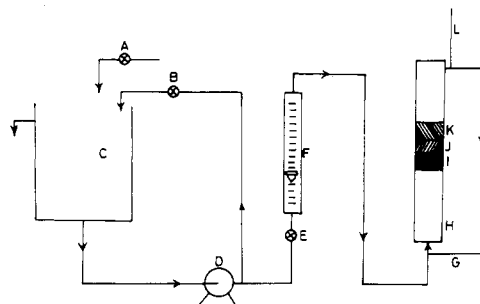


Figure 1. Sketch of experimental setup

- A, B, E: Needle valves
- G, L: Thermometer
- C: Stainless-steel constant head tank
- H: Test column
- I, K: Bed of glass beads
- D: All bronze centrifugal pump
- J: Bed of active solute particles
- F: Rotameter

¹ To whom correspondence should be addressed.

between the two glass bead beds, and water circulation was maintained at a known flow rate for a known interval of time. Five minutes was allowed to attain equilibrium, and the three samples of the outgoing stream were collected within the next 10–15 min. The volume of the liquid sampled in each case was of the order of 200–300 ml. These were then analyzed for the acid concentration by titration with 0.010*N* NaOH solution using phenol red as the indicator. Measurements of the pellet bed length and inlet and outlet water temperatures were also taken. Solute pellets were changed after every two runs. For all the runs made under these sets, the fluid used was distilled water.

The titrimetric method failed to give reliable end-points at higher flow rates, as encountered in the fluidizing region because of the low acid concentrations involved. Hence, a second set of measurements was made with all the pellet sizes by measuring the loss in weight of the bed during a known interval of time at a known flow rate. The reliability of this method was tested in a separate series of runs performed at low flow rates by calculating the transfer rates from the measured weight losses and from the concentrations determined by the titrimetric method. The calculated values agreed fairly well, and the difference was less than 2%.

The bed retaining screen and the top bed of glass beads were removed to have free expansion of the bed. After arranging the apparatus in the proper manner, the lower bed of glass beads was formed, and its upper surface was made smooth and horizontal. The solute particles weighed to the nearest 0.05 mg were now charged through the top opening of the test column which was partially filled with water to prevent particle breakage. The flow of water was maintained at a known rate for a known interval of time. The measurements of the pellet bed height and outlet water temperatures were also made.

After the run, the flow of water was terminated, and the bed was taken out of the test column. It was dried in a desiccator to constant weight and reweighed. The weight loss so obtained was used to evaluate the mass-transfer rate. Fresh particles were used for each run. Depending upon the flow rate, each run lasted for a period of 10–20 min. In a separate experiment, the loss in weight during the charging of the particles in the test column and during their removal from it was determined and was negligible in comparison to the total weight loss encountered during a run. However, the final weight losses were corrected by subtracting these values. Because of the inadequate supply of the distilled water, all the runs under this set were made with tap water.

In all the runs the acid concentration in the inlet stream was always zero. The mass-transfer coefficient, k_c , was calculated by the equation:

$$V(C_2 - C_1) = k_c S (\Delta C)_{lm} \quad (4)$$

or

$$k_c = (V/S) \cdot \ln(C_s/C_s - C_2) \quad (5)$$

The mass-transfer coefficient was then converted into the J_d and J_d' factor given by the equations:

$$J_d = \frac{k_c}{u} N_{Sc}^{2/3} \quad (6)$$

$$J_d' = \frac{k_c}{u} N_{Sc}^{0.58} \quad (7)$$

The particle Reynolds numbers were calculated by Equations 1–3. The required physical properties were evaluated at the mean temperature of the measurement from the graphs prepared for the purpose by use of reported

literature values. The solubility data used in the calculations were taken from the literature (5, 15, 16, 19, 20). Because of the divergent nature of the reported diffusivities, the same were computed with Wilke and Chang's relation (23). The viscosity data of water used in the calculations were taken from Perry's Handbook (12).

The range of the values of the various quantities covered in the present work is given in Table II. A summary of the experimental and derived quantities for typical runs is given in Table III.

Results and Discussion

The variation of the mass-transfer coefficient, k_c , with the modified Reynolds number, N_{Re}'' , is shown in Figure 3. The results fall on separate and nearly parallel lines for

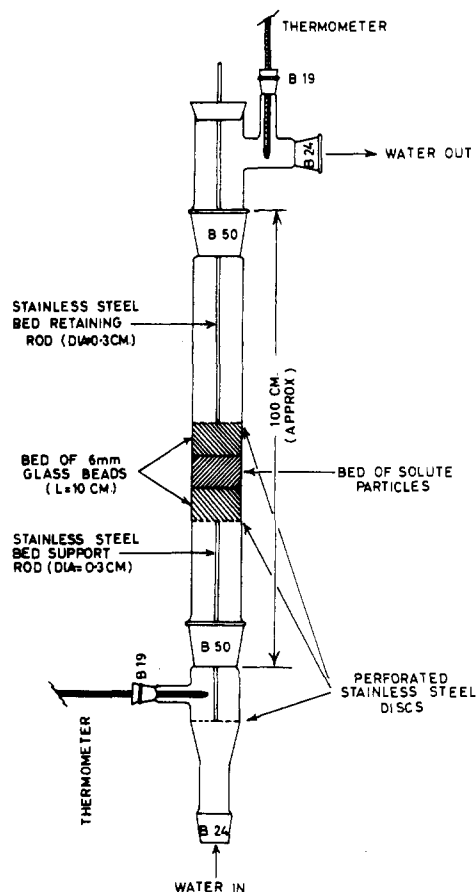


Figure 2. Details of test column

Table II. Range of Present Observations

Quantity	Range
Number of observations	204
Particle diameter, cm	0.5961–1.1968
Particle shape	Dished-end and flat-end cylindrical pellets
Column diameter, cm	3.901–7.22
Temperature, °C	19.4–34.8
Flow velocity, cm/sec	0.003262–12.38
Fixed bed height, cm	2.3–11.4
Void fraction	0.2698–0.9053
$k_c \times 10^4$, cm/sec	1.762–71.69
J_d	0.03570–4.18
N_{Bo}	572–1350
N_{Re}''	0.405–11,610

Table III. Experimental Data and Derived Quantities for Typical Runs

Run no. 1	T, °C 2	L, cm 3	ϵ 4	$C_2 \times 10^2$, g/l. 5	$D_p G$	$k_c \times 10^4$, cm/sec 7	J_d 8
					$\mu(1 - \epsilon)$ 6		
Fixed bed							
$D_p = 1.121$ cm, $D_c = 3.901$ cm, $W = 100.0 \pm 0.10$ g							
I-1	31.2	11.40	0.4341	34.52	535.7	30.23	0.1093
I-2	31.2	11.40	0.4341	30.92	803.4	40.53	0.09819
I-3	31.1	11.40	0.4341	24.31	1071	42.00	0.07633
I-4	31.1	11.40	0.4341	19.72	1340	42.42	0.06167
I-5	31.1	11.40	0.4341	18.99	1609	49.17	0.05958
I-6	31.1	11.40	0.4341	17.16	2143	59.00	0.05359
I-7	31.1	11.40	0.4341	16.82	2409	64.85	0.05238
$D_p = 1.121$ cm, $D_c = 4.558$ cm, $W = 52.98 \pm 0.10$ g							
II-11	24.2	4.50	0.4389	16.47	135.5	13.39	0.2310
II-12	21.8	4.50	0.4389	11.92	160.6	12.93	0.1854
II-13	19.4	4.50	0.4389	8.330	304.4	19.39	0.1530
II-14	24.6	4.50	0.4389	8.087	514.1	24.00	0.1030
II-15	22.5	4.50	0.4389	6.198	653.0	26.16	0.09139
$D_p = 0.8973$ cm, $D_c = 4.558$ cm, $W = 29.52 \pm 0.10$ g							
II-17	20.4	2.70	0.4889	10.65	72.67	11.14	0.3174
II-18	21.2	2.70	0.4889	8.539	111.0	12.94	0.2382
II-19	21.8	2.70	0.4889	8.385	141.3	15.56	0.2227
II-20	25.1	2.70	0.4889	5.417	304.9	18.09	0.1133
II-21	25.2	2.70	0.4889	5.380	458.1	26.73	0.1113
$D_p = 0.8569$ cm, $D_c = 4.558$ cm, $W = 31.30 \pm 0.10$ g							
II-22	21.6	2.30	0.3584	16.01	30.70	8.742	0.4406
II-23	22.8	2.30	0.3584	13.58	58.72	13.20	0.3419
II-24	23.7	2.30	0.3584	10.13	89.62	14.15	0.2368
$D_p = 0.8061$ cm, $D_c = 3.901$ cm, $W = 75.00 \pm 0.10$ g							
I-33	30.0	7.90	0.3890	46.80	174.8	26.02	0.1957
I-34	30.0	7.90	0.3890	35.12	349.5	38.71	0.1456
I-35	30.0	7.90	0.3890	24.17	524.4	39.52	0.09881
I-36	30.0	7.90	0.3890	22.19	699.0	48.17	0.09057
I-37	30.0	7.90	0.3890	18.64	874.0	50.27	0.07561
I-38	30.0	7.90	0.3890	16.96	1048	54.92	0.06887
I-39	30.0	7.90	0.3890	16.57	1399	71.69	0.06738
I-40	30.4	11.0 ^a	0.4147	18.55	1470	59.06	0.05489
I-45	30.4	11.0 ^a	0.4147	17.08	1856	67.81	0.05046
$D_p = 0.8061$ cm, $D_c = 4.558$ cm, $W = 37.00 \pm 0.10$ g							
II-47	21.5	2.50	0.2698	22.06	25.26	8.884	0.4514
II-48	25.0	2.50	0.2698	18.69	51.01	12.45	0.2943
II-49	25.9	2.50	0.2698	17.31	77.85	16.99	0.2584
II-50	23.3	2.50	0.2598	4.817	368.1	24.67	0.1270
$D_p = 0.7743$ cm, $D_c = 3.901$ cm, $W = 75.00 \pm 0.10$ g							
I-51	29.9	9.00	0.4636	48.20	190.4	23.15	0.1762
I-52	30.2	9.00	0.4636	36.59	383.1	34.55	0.1293
I-53	30.0	9.00	0.4636	32.35	572.8	46.00	0.1152
I-54	30.0	9.00	0.4636	31.07	763.5	58.65	0.1103
I-55	30.0	9.00	0.4636	27.32	954.5	64.00	0.09635
I-56	30.0	9.00	0.4636	23.67	1145	66.52	0.08350
I-57	30.0	9.00	0.4636	21.70	1337	70.80	0.07615
$D_p = 0.7743$ cm, $D_c = 4.558$ cm, $W = 32.16 \pm 0.10$ g							
II-58	21.2	3.00	0.4949	19.54	34.91	8.130	0.4166
II-59	21.9	3.00	0.4949	15.55	65.94	11.70	0.3137
II-60	21.9	3.00	0.4949	12.69	98.58	14.23	0.2554
II-61	23.9	3.00	0.4949	11.84	129.5	15.45	0.2043
II-62	23.1	3.00	0.4949	8.513	254.2	22.73	0.1555
III-63	24.6	3.00	0.4949	6.965	395.0	26.91	0.1155
II-64	23.7	3.00	0.4949	7.352	386.8	29.00	0.1291
$D_p = 0.5961$ cm, $D_c = 4.558$ cm, $W = 22.71 \pm 0.10$ g							
II-66	22.5	2.30	0.5060	12.25	78.74	17.07	0.2990
II-67	25.9	2.30	0.5060	12.27	106.7	19.24	0.2344
II-68	23.3	2.30	0.5060	8.598	201.2	29.13	0.1975

Table III. Continued

Run no. 1	$T, ^\circ\text{C}$ 2	L, cm 3	ϵ 4	$C_2 \times 10^2, \text{g/l.}$ 5	$D_p G$		$k_c \times 10^4, \text{cm/sec}$ 7	J_d 8
					$\mu(1 - \epsilon)$ 6			
Fixed bed								
$D_p = 0.5961 \text{ cm}, D_c = 7.22 \text{ cm}, W = 67.20 \pm 0.10 \text{ g}$								
III-76	32.7	2.20	0.3923	219.5	2.010		5.492	2.506
III-77	29.6	2.20	0.3923	141.2	1.995		3.765	1.830
III-78	30.5	2.20	0.3923	172.1	2.230		5.652	2.438
III-79	29.6	2.20	0.3923	133.5	2.640		4.771	1.775
III-80	30.6	2.20	0.3923	108.4	3.308		4.506	1.305
III-81	30.3	2.20	0.3923	84.8	5.340		5.828	1.052
III-82	30.8	2.20	0.3923	32.8	24.35		8.640	0.3359
Fluidized bed								
$D_p = 1.121 \text{ cm}, D_c = 4.558 \text{ cm}, W = 52.98 \pm 0.10 \text{ g}$								
II-1	21.8	5.20	0.5144	5.462	928.1		29.62	0.08498
II-2	26.4	5.90	0.5720	5.732	1403		36.93	0.07305
II-3	26.3	6.50	0.6114	5.669	1796		36.63	0.06232
II-4	26.4	7.00	0.6392	4.960	2219		36.93	0.05479
II-5	25.4	7.50	0.6633	4.616	2617		39.47	0.05438
II-6	24.6	8.00	0.6844	3.783	3047		36.93	0.04756
II-7	22.9	9.50	0.7341	2.986	4176		36.93	0.04238
$D_p = 0.8973 \text{ cm}, D_c = 4.558 \text{ cm}, W = 29.52 \pm 0.10 \text{ g}$								
II-8	25.3	3.00	0.5399	4.270	680.6		28.73	0.08933
II-9	24.5	4.00	0.6551	3.563	1338		36.71	0.07907
II-10	26.8	4.50	0.6933	3.906	1845		42.84	0.07152
II-11	26.8	5.20	0.7355	3.534	2436		43.62	0.06374
II-14	24.1	6.00	0.7700	2.673	3312		46.55	0.06096
II-15	27.5	7.00	0.8028	2.993	4888		54.26	0.05120
II-16	22.9	9.00	0.8467	2.150	6763		52.12	0.05126
II-17	23.0	13.50	0.8978	1.689	11610		46.80	0.04018
$D_p = 0.8569 \text{ cm}, D_c = 4.558 \text{ cm}, W = 31.30 \pm 0.10 \text{ g}$								
II-18	26.1	2.80	0.4730	3.451	721.6		27.79	0.06850
II-19	24.6	3.10	0.5240	3.566	927.9		34.15	0.07331
II-20	21.9	3.50	0.5784	2.698	1148		34.29	0.07006
II-21	25.2	4.30	0.6568	2.981	1738		39.17	0.06116
II-22	26.2	5.00	0.7049	2.868	2325		41.69	0.05539
II-23	24.6	5.70	0.7411	2.590	2845		43.67	0.05626
$D_p = 0.8061 \text{ cm}, D_c = 4.558 \text{ cm}, W = 37.00 \pm 0.10 \text{ g}$								
II-25	24.8	3.60	0.4930	4.634	823.0		33.54	0.07127
II-26	21.9	4.30	0.5756	3.499	1072		32.38	0.06621
II-27	25.7	5.90	0.6907	4.132	1835		38.55	0.05889
II-28	26.3	7.00	0.7393	3.814	2480		39.12	0.05165
II-29	24.6	8.00	0.7719	3.305	3035		40.47	0.06213
II-30	22.9	9.20	0.8016	2.549	4027		37.29	0.04280
$D_p = 0.7743 \text{ cm}, D_c = 4.558 \text{ cm}, W = 32.16 \pm 0.10 \text{ g}$								
II-32	25.4	3.30	0.5409	6.378	589.1		31.50	0.09763
II-33	23.2	4.00	0.6213	4.522	1021		35.89	0.08136
II-34	23.6	4.80	0.6844	3.956	1442		36.99	0.07069
II-35	23.9	5.30	0.7141	3.799	1831		39.07	0.06460
II-36	25.5	6.00	0.7496	3.670	2417		40.36	0.05544
II-37	24.4	7.00	0.8736	3.092	3058		39.87	0.05160
II-38	27.3	9.00	0.8316	2.667	5030		38.28	0.03641
II-39	22.9	11.00	0.8591	2.015	6351		36.27	0.03570
$D_p = 0.5961 \text{ cm}, D_c = 4.558 \text{ cm}, W = 22.71 \pm 0.10 \text{ g}$								
II-40	23.3	2.50	0.5456	6.982	327.9		35.71	0.1614
II-41	23.1	2.80	0.5942	4.868	487.2		33.94	0.1165
II-42	21.1	3.00	0.6213	4.025	622.0		36.09	0.1069
II-43	22.5	3.60	0.6844	3.989	927.0		41.03	0.09588
II-44	22.9	4.20	0.7295	3.488	1275		41.67	0.08219
II-45	23.3	4.80	0.7633	3.274	1679		44.58	0.07558
II-46	23.4	5.60	0.7971	2.882	2209		44.44	0.06677
II-47	24.1	6.50	0.8252	2.643	2894		43.05	0.05639
II-48	27.5	8.00	0.8580	2.916	4607		50.14	0.04732

^a $W = 100.00 \pm 0.10 \text{ grams.}$

each particle size. These plots indicate that in the fixed bed region, the mass-transfer coefficient increases with increasing modified Reynolds number and decreasing particle size. The fluidized bed values are essentially independent of the modified Reynolds number and show an increase with decreasing particle size; however, this increase is very much less than in the fixed bed region. The fluidized bed mass-transfer coefficients are, for the same modified Reynolds number, lower than the corresponding fixed bed mass-transfer coefficients. The dependence of the fixed bed k_c values on the N_{Re}'' can be represented by the equation:

$$k_c = f(N_{Re}'')^{0.525} \quad (8)$$

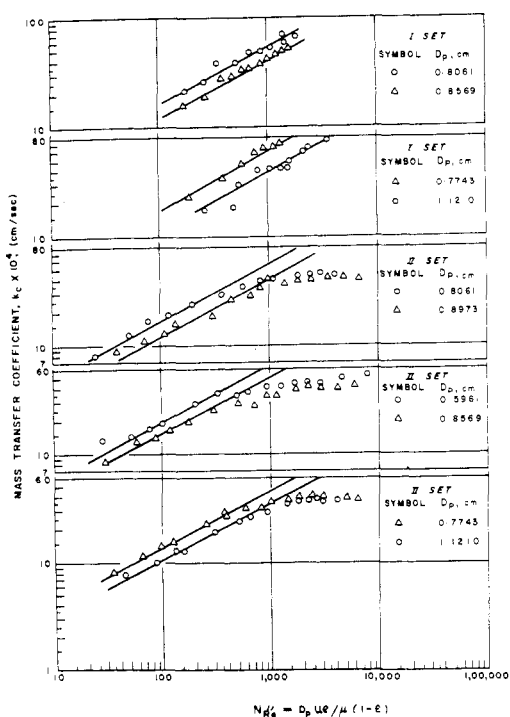


Figure 3. Effect of particle size on mass-transfer coefficient, k_c

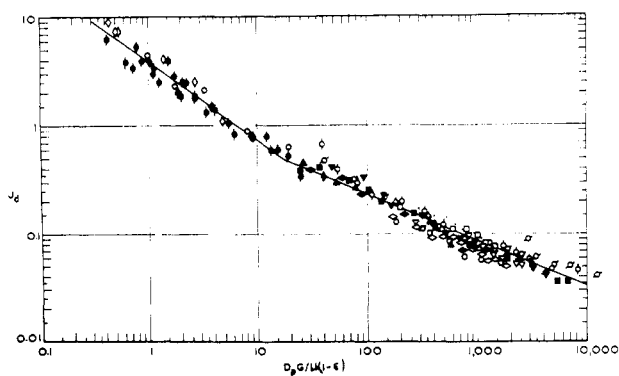


Figure 4. J_d vs. N_{Re}'' plot. Dissolution of benzoic acid into water

Benzoic acid			D_p , cm
I	II	III	
—	—	◆	1.1968
▽	▼	—	1.1210
—	○	—	0.8973
—	—	○	0.8701
—	◆	○	0.8569
—	—	○	0.8517
—	—	○	0.8505
△	▲	○	0.8061
□	■	○	0.7743
—	○	●	0.5961

● also includes Set IV data

In Figure 4, the J_d factor data for both fixed and fluidized beds are plotted vs. particle Reynolds number, N_{Re}'' , as a typical case. No effect of the particle shape and size and column diameter is seen on such a plot. This plot is also independent of the fixed bed height which varied from 1.0 to 11.4 cm. From this plot one finds that the results can be expressed by two separate expressions of the form:

$$J_d = A(N_{Re}'')^{-B} \quad (9)$$

One is for the low N_{Re}'' (<20.0), and other for the higher (>20.0). The least-squares regression gave

$$J_d = 3.713(N_{Re}'')^{-0.7131} \quad (10)$$

for $N_{Re}'' < 20.0$ with an average deviation of $\pm 15.5\%$ and

$$J_d = 1.8603(N_{Re}'')^{-0.4514} \quad (11)$$

for $N_{Re}'' > 20.0$ with an average deviation of $\pm 12.75\%$.

To compare the present results with those published and to find a more general relation applicable to random packed and fluidized beds of various types of particles, the present data together with those of others (1, 4, 6-8, 11, 18, 22, 24, 25) were analyzed collectively and are plotted in Figure 5 as a J_d vs. N_{Re}'' plot. This plot shows the close agreement between the present and published data. In correlating the heat and mass-transfer data for particle fluid systems, the influence of the bed voidage has been considered by many (9-11, 13, 14, 17, 25). Gupta et al. (9), Sengupta and Thodos (17), and Wilson and Geankoplis (25) have shown that

$$J_d \text{ (or } J_h) \propto (1/\epsilon) \quad (12)$$

Pfeffer (13) and Ruckenstein (14) have shown that the function on the right-hand side of Equation 12 is a complex function of bed voidage. Wilson and Geankoplis (25) have pointed out that Pfeffer's function can be safely approximated to Equation 12 without involving much error. Ruckenstein has also shown that his complex bed voidage function too can be approximated to

$$J_d \text{ (or } J_h) \propto \epsilon^{-1.15} \quad (13)$$

Malling and Thodos (10), using the gas-phase data, found that

$$J_d \text{ (or } J_h) \propto \epsilon^{-1.19} \quad (14)$$

To test the validity of these conclusions and to verify the exponent on the Schmidt group, the least-squares analysis of the entire data was made taking combinations of one of the J_d , ϵJ_d , $\epsilon^{1.19} J_d$, $\epsilon^{1.15} J_d$, J_d' , $\epsilon J_d'$, $\epsilon^{1.19} J_d'$, and $\epsilon^{1.15} J_d'$ with one of the three particle Reynolds numbers at a time. The entire data were divided into two groups, one for $N_{Re}'' < 20.0$ and the other for $N_{Re}'' > 20.0$. This division is purely arbitrary, and no theoretical importance can be attached to $N_{Re}'' = 20.0$. The data in the above two groups were processed separately, and best values of constants A and B and the average deviations were calculated in each case. Comparing the average deviation for the various situations one finds that equations

$$J_d = 3.8155(N_{Re}'')^{-0.7313}, \text{ for } N_{Re}'' < 20.0 \quad (15)$$

and

$$J_d = 1.6218(N_{Re}'')^{-0.4447}, \text{ for } N_{Re}'' > 20.0 \quad (16)$$

correlate the entire data successfully with least deviation. The average deviations for the two cases are ± 22.47 and $\pm 14.13\%$, respectively. The deviation of the experimental data from

$$J_d' = 1.9020(N_{Re}'')^{-0.6976}, \text{ for } N_{Re}'' < 20.0 \quad (17)$$

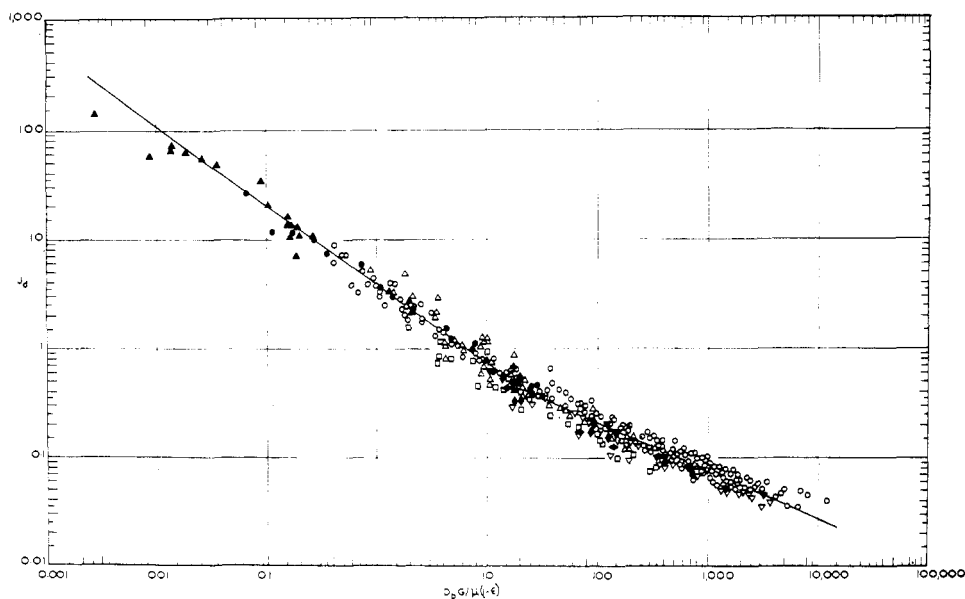


Figure 5. Solid-liquid mass transfer in fixed and fluidized beds. J_d' vs. N_{Re}'' plot

- | | | | |
|---|---------------------------|---|----------------------------------|
| ▽ | McCune and Wilhelm (1949) | ◆ | Venkateswaran and Laddha (1966) |
| △ | Gaffney and Drew (1950) | ▲ | Wilson and Geankoplis (1966) |
| □ | Evans and Gerald (1953) | ▼ | Bhattacharya and Raja Rao (1967) |
| · | Dunn et al. (1956) | ■ | Snowden and Turner (1967) |
| ◆ | Fan et al. (1960) | ○ | Present study |
| ● | Williamson et al. (1963) | | |

and

$$J_d' = 0.8890 (N_{Re}'')^{-0.4469}, \text{ for } N_{Re}'' > 20.0 \quad (18)$$

are ± 18.54 and 13.80% , respectively. The deviations are better than those for J_d and thus favor 0.58 as the exponent for the Schmidt group; however, the improvement is not that marked to clarify the situation completely, and it needs some more work. Further, the inclusion of ϵ , $\epsilon^{1.15}$, or $\epsilon^{1.19}$ with the J_d or J_d' factor does not improve the deviation and thus shows that for correlating the random packed and fluidized bed data, it is not necessary to modify the mass-transfer factor by including a bed voidage term.

Conclusions

On the basis of the results presented, it can be concluded that for the same Reynolds number, the mass-transfer coefficient increases with decreasing particle size in both fixed and fluidized beds. In the fixed bed the mass-transfer coefficient increases with the increasing Reynolds number, whereas in the fluidized bed it remains fairly constant. At a given Reynolds number, the fixed bed values are always higher than the corresponding fluidized bed values. The entire liquid-phase data can be successfully correlated by the equations:

$$J_d = 3.8155 (N_{Re}'')^{-0.7313}, \text{ for } N_{Re}'' < 20.0$$

and

$$J_d = 1.6218 (N_{Re}'')^{-0.4447}, \text{ for } N_{Re}'' > 20.0$$

without the use of a modifying void fraction term with the mass-transfer factor. The above two equations are valid for a N_{Re}'' range of 0.01–12000, a Schmidt number range of 572–70,000, and void fraction range of 0.2698–0.9653.

Acknowledgment

The authors wish to express their appreciation to the Electrical Engineering Department Institute of Technology, Banaras Hindu University, for providing the computational facilities.

Nomenclature

- A = constant, dimensionless
 A_c = cross section of the bed, L^2
 A_p = geometric surface area of a particle, L^2
 B = constant, dimensionless
 C_s = saturation concentration, M/L^3
 C_1 = inlet concentration, M/L^3
 C_2 = outlet concentration, M/L^3
 $(\Delta C)_{lm}$ = log mean concentration difference, M/L^3
 C_p = heat capacity, L^2/t^2T
 D = molecular diffusion coefficient, L^2/t
 D_c = column diameter, L
 D_p = particle diameter, L
 f = a function
 G = mass flow rate, M/L^2t
 h = heat-transfer coefficient, M/t^3T
 J_d = mass-transfer factor = $(k_c/u) N_{Sc}^{2/3}$, dimensionless
 J_d' = mass-transfer factor = $(k_c/u) N_{Sc}^{0.58}$, dimensionless
 J_h = heat-transfer factor = $(h/C_pG) (\mu C_p/k)^{2/3}$, dimensionless
 k_c = mass-transfer coefficient, L/t
 k = thermal conductivity, ML/t^3T
 \ln = natural logarithm
 L = length, L
 L = bed height, L
 M = mass, M
 N_{Re} = particle Reynolds number = D_pG/μ , dimensionless
 N_{Re}' = particle Reynolds number = $D_pG/\mu\epsilon$, dimensionless
 N_{Re}'' = particle Reynolds number = $D_pG/\mu(1 - \epsilon)$, dimensionless
 N_{Sc} = Schmidt number = $\mu/\rho D$, dimensionless
 S = total effective surface area of particles in the bed, L^2
 t = time, t
 T = temperature, T
 u = flow velocity, L/t

V = volumetric flow rate; L^3/t
 W = total weight of particles in the bed, M
 Δ = operator indicating a change
 ϵ = void fraction = $1 - (W/A_c L \rho_s)$, dimensionless
 μ = viscosity, M/Lt
 ρ = density, M/L³
 ρ_s = density of solid, M/L³

Literature Cited

- (1) Bhattacharya, S. N., Raja Rao, M., *Indian Chem. Eng.*, **9**, Trans. 65 (1967).
- (2) Chilton, T. H., Colburn, A. P., *Ind. Eng. Chem.*, **26**, 1183 (1934).
- (3) Dryden, C. E., Strang, D. A., Withrow, A. E., *Chem. Eng. Progr.*, **49**, 141 (1953).
- (4) Dunn, W. E., Bonilla, C. F., Ferstenberg, C., Gröss, B., *AIChE J.*, **2**, 184 (1956).
- (5) Eisenberg, M., Chang, P., Tobias, C. W., Wilke, C. R., *ibid.*, **1**, 558 (1955).
- (6) Evans, G. C., Gerald, C. F., *Chem. Eng. Progr.*, **49**, 135 (1953).
- (7) Fan, L. T., Yang, Y. C., Wen, C. Y., *AIChE J.*, **6**, 482 (1960).
- (8) Gaffney, B. J., Drew, T. B., *Ind. Eng. Chem.*, **42**, 1120 (1950).
- (9) Gupta, S. N., Chaubey, R. B., Upadhyay, S. N., *Chem. Eng. Sci.*, **29**, 839 (1974).
- (10) Malling, G. F., Thodos, G., *Int. J. Heat Mass Transfer*, **10**, 489 (1967).
- (11) McCune, L. K., Wilhelm, R. H., *Ind. Eng. Chem.*, **41**, 1124 (1949).
- (12) Perry, J. H., "Chemical Engineer's Handbook," 4th ed., McGraw-Hill, New York, N.Y., 1963.
- (13) Pfeffer, R., *Ind. Eng. Chem. Fundam.*, **3**, 380 (1964).
- (14) Ruckenstein, E., *Z. Priklad Khim.*, **35**, 377 (1962).
- (15) Seidell, A., "Solubilities of Inorganic and Organic Compounds," 3rd ed., Vol II, Van Nostrand, New York, N.Y., 1941.
- (16) Seidell, A., Linke, W. F., *ibid.*, Supplement to 3rd ed., 1952.
- (17) Sengupta, A., Thodos, G., *Chem. Eng. Progr.*, **58**, (7), 58 (1962).
- (18) Snowden, C. B., Turner, J. C. R., Proceedings of International Symposium on Fluidization, A. A. H. Drinkenberg, Ed., pp 599-608, Eindhoven, The Netherlands, 1967.
- (19) Steele, L. R., Geankoplis, C. J., *AIChE J.*, **5**, 178 (1959).
- (20) Stephen, H., Stephen, T., "Solubilities of Inorganic and Organic Compounds," Pergamon Press, New York, N.Y., 1963.
- (21) Upadhyay, S. N., Tripathi, G., *J. Sci. Ind. Res.*, in press (1974).
- (22) Venkateswaran, S. D., Laddha, G. S., *Indian Chem. Eng.*, **8**, Trans. 333 (1966).
- (23) Wilke, C. R., Chang, P., *AIChE J.*, **1**, 264 (1955).
- (24) Williamson, J. E., Bazaire, K. E., Geankoplis, C. J., *Ind. Eng. Chem. Fundam.*, **2**, 126 (1963).
- (25) Wilson, E. J., Geankoplis, C. J., *ibid.*, **5**, 9 (1966).

Received for review August 4, 1971. Resubmitted April 19, 1974. Accepted September 3, 1974.

Mass-Transfer Coefficient and Pressure-Drop Data of Two-Phase Oxygen-Water Flow in Bubble Column Packed with Static Mixers

Liang T. Fan,¹ Hsiu H. Hsu, and Kang B. Wang

Department of Chemical Engineering, Kansas State University, Manhattan, Kan. 66506

The mass-transfer coefficient and pressure-drop data of an oxygen-water flow system through a bubble column packed with static mixers (Koch type) are presented. Compared with the data of an unpacked column, the results show that the mass-transfer coefficient is almost doubled, while the pressure drop only increases slightly. A bubble column packed with the static mixers appears to be effective in aeration or oxygenation systems; thus, the data presented here should be of practical value.

The versatility of static mixers has been recognized in recent years (3, 4). Several different types of static mixers are available on the market. Among them, the Koch (or Sulzer) static mixer is the latest design. The Koch static mixer may be suitable for use in an aeration or oxygenation system. This communication presents some results on measurements of oxygen transfer rate and pressure drop in a bubble column packed with the static mixers.

The static mixer is constructed of layers of corrugated sheet metal (Figure 1) or plastics. When oxygen passes through the static mixer concurrently with water flow, small and uniform bubbles are generated as can be seen in Figure 2. These bubbles mix thoroughly with water through open and intersecting channels of the static mixer. The rate of oxygen absorption by water should be highly enhanced through the combined effect of increased interfacial surface area, effective radial mixing, and lengthened gas-liquid contact time. However, the in-

crease in pressure drop through the static mixer over the same size of unpacked column should not be excessive because of the uniformity, geometrical simplicity, and relatively large number and magnitude of channel openings in the mixer unit.

Experimental

The schematic diagram of the apparatus is shown in Figure 3. Koch static mixers with spacers were packed in the bubble column of 4-in. diameter. Tap water was pumped from a water tank through a rotameter to the bottom of the column. Oxygen from an oxygen cylinder flowed through another rotameter to a $3/4$ -in. nozzle at the bottom of the bubble column.

Dissolved oxygen concentrations at the bottom and top of the bubble column were measured by using a galvanic cell oxygen analyzer marketed by the Precision Scientific

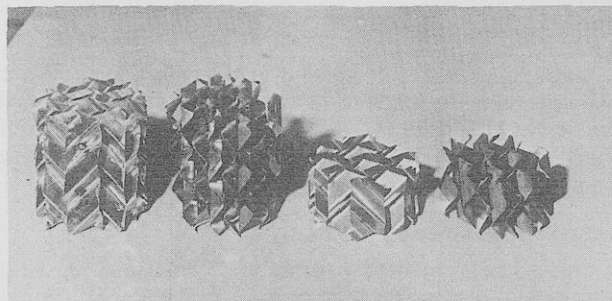


Figure 1. Koch static mixer AY type, whole element ($l/D = 1$) and half element ($l/D = 1/2$), $D = 4$ in.

¹ To whom correspondence should be addressed.